Protective Role of miR-34c in Hypoxia by Activating Autophagy through BCL2 Repression

Soyoung Kim[1], Jaeseok Han[1,2], Young-Ho Ahn[3], Chang Hoon Ha[1], Jung Jin Hwang[1], Sang-Eun Lee[4], Jae-Joong Kim[4,*], and Nayoung Kim[1,*]

[1]Department of Convergence Medicine & Asan Institute for Life Sciences, Asan Medical Center, University of Ulsan College of Medicine, Seoul 05505, Korea, [2]Asan Medical Institute for Convergence Science and Technology, Asan Medical Center, University of Ulsan College of Medicine, Seoul 05505, Korea, [3]Department of Molecular Medicine, College of Medicine, Ewha Womans University, Seoul 07804, Korea, [4]Division of Cardiology, Department of Internal Medicine, Asan Medical Center, University of Ulsan College of Medicine, Seoul 05505, Korea
*Correspondence: naykim@amc.seoul.kr (NK); jjkim@amc.seoul.kr (JJK)
https://doi.org/10.14348/molcells.2022.2010
www.molcells.org

Hypoxia leads to significant cellular stress that has diverse pathological consequences such as cardiovascular diseases and cancers. MicroRNAs (miRNAs) are one of regulators of the adaptive pathway in hypoxia. We identified a hypoxia-induced miRNA, miR-34c, that was significantly upregulated in hypoxic human umbilical cord vein endothelial cells (HUVECs) and in murine blood vessels on day 3 of hindlimb ischemia (HLI). miR-34c directly inhibited BCL2 expression, acting as a toggle switch between apoptosis and autophagy *in vitro* and *in vivo*. BCL2 repression by miR-34c activated autophagy, which was evaluated by the expression of LC3-II. Overexpression of miR-34c inhibited apoptosis in HUVEC as well as in a murine model of HLI, and increased cell viability in HUVEC. Importantly, the number of viable cells in the blood vessels following HLI was increased by miR-34c overexpression. Collectively, our findings show that miR-34c plays a protective role in hypoxia, suggesting a novel therapeutic target for hypoxic and ischemic diseases in the blood vessels.

Keywords: autophagy, BCL2, hypoxia, ischemia, miR-34c

INTRODUCTION

Decreased blood flow results in hypoxia, leading to the diseases including stroke (cerebral ischemia), heart infarction (myocardial ischemia), and tumor angiogenesis (Michiels, 2004). MicroRNAs (miRNAs) are small regulatory RNAs that repress gene expression by directly binding to the 3′ untranslated region (UTR) of target mRNA (Bushati and Cohen, 2007). miRNAs are key regulators in cellular processes including stress responses in the cardiovascular system, such as hypoxia (Akkoc and Gozuacik, 2020) and arrhythmia (Guo et al., 2022). Under hypoxic conditions, several miRNAs, such as miR-21 and miR-34a, are known to be upregulated through enhancing the biogenesis of miRNAs and then inhibit the expression of target mRNAs involved in cell metabolism such as angiogenesis and apoptosis (Chen et al., 2013; Nallamshetty et al., 2013; Zhou et al., 2013).

Autophagy is a defense pathway from physiological stimuli including hypoxic/ischemic stress. Autophagy is a self-degradative system that is a critical pathway for clearing damaged organelles and removing intracellular aggregates (Glick et al., 2010; Marino et al., 2014). This process is mainly stimulated by nonlethal cellular stresses (Glick et al., 2010; Lee et al., 2020b) and consequently induces lysosomal deg-

radation through the formation of autophagosomes and autolysosomes (Glick et al., 2010; Mizushima et al., 2010). Among the key regulators of autophagic flux, BCL2 inhibits autophagy as it directly interacts with Beclin-1 (ATG6) which is a critical factor in the regulation of autophagosome formation (Fernandez et al., 2018; Marquez and Xu, 2012). Microtubule-associated protein light chain 3 (LC3), a member of the ATG8 protein family, is widely used to monitor cellular autophagy. LC3-II is converted from a cytosolic LC3-I that conjugated with phosphatidylethanolamine, which is recruited and formed autophagosomes (Jang et al., 2020). The amount of LC3-II and the extent of LC3 conversion (LC3-I to LC3-II) are regarded as indicators of autophagy activity (Gustafsson and Gottlieb, 2009). Cardiac ischemia causes upregulation of autophagy as assessed by increased LC3-II and Beclin-1, leading to cardioprotection (Gurusamy et al., 2009). The ubiquitin-binding protein p62 (Sequestosome-1) links the autophagy pathway and the ubiquitin–proteasome system upon ubiquitinated protein degradation (Liu et al., 2016). Since several studies have reported that increased induction of autophagy is required for the survival of hypoxic cells (Bellot et al., 2009; Tan et al., 2016; Zhang et al., 2008), autophagy can play a protective role for cells undergoing hypoxia-induced stress. Nevertheless, the molecular mechanism that hypoxia promotes autophagic activity has not been fully understood in cardiovascular diseases.

Herein, we identified a new hypoxia-induced miRNA, miR-34c-5p, which is a major form of miR-34c, both *in vitro* and *in vivo* by using human umbilical cord vein endothelial cell (HUVEC) lines and a mouse hindlimb ischemia (HLI) model, respectively. During hypoxia, HUVEC lines significantly reduced the caspase 3/7 activity and increased cell viability, as well as induced autophagy. Based on the computational prediction, miR-34c directly repressed BCL2 which acts as a toggle switch regulating autophagy/apoptosis (Marquez and Xu, 2012). Furthermore, miR-34c-mediated BCL2 repression can activate autophagy in hypoxic HUVECs and mouse hindlimb ischemic vessels. Our findings suggest that miR-34c have a protective role against hypoxic stress and that miR-34c could be a novel biomarker for hypoxia-related diseases.

MATERIALS AND METHODS

Cell culture
HUVECs were purchased from Lonza (Switzerland) and cultured in EGM-2 media supplemented with 2% fetal bovine serum (FBS) and an EGM-2 Bullet Kit (Lonza). For the experiments, HUVECs were used between passages 5-9. HEK293T cells (ATCC, USA) were maintained in Dulbecco's modified Eagle's medium (DMEM; Hyclone, USA) supplemented with 10% FBS, 100 U/ml penicillin, and 100 μg/ml streptomycin (Corning, USA).

To induce hypoxia, HUVECs were seeded in 100-mm dishes one day prior to induction. HUVECs were incubated in a hypoxic chamber (1% O_2, 5% CO_2, and 90% N_2) for 24 h and 72 h. Alternatively, HUVECs were treated with hydrogen peroxide (H_2O_2; i.e., dysoxia) (Sigma-Aldrich, USA) at 700 nM for 24 h.

Murine HLI model
A murine model of HLI was set up in 8- to 12-week-old C57BL/6 mice (OrientBio, Korea). The mock control or miR-34c-expressing lentivirus was injected through the tail vein at a dose of 4 μg/mouse in 0.2 ml of phosphate-buffered saline (PBS) once a day for three consecutive days, followed by performing HLI on day 2. To establish the HLI mouse model, mice were anesthetized with a mixture of tiletamine and zolazepam (Zoletil 50; Virbac, Korea) and xylazine (Rompun; Bayer Korea, Korea) following standard protocols. The superficial femoral artery was ligated with 5-0 polypropylene silk suture (Ethicon, USA), and the skin was closed. Mice were sacrificed after 3 days, and the vessels were harvested. For sham control, the procedures were performed except ischemia by ligation. All the procedures were approved by the Institutional Animal Care and Use Committee (IACUC) of Asan Medical Center (approval No. 2018-12-216).

For H&E histological staining, the vessels were fixed in 4% formalin overnight. The vessel samples were processed and embedded in paraffin and stained with H&E by the Comparative Pathology Core Facility, Convergence Medicine Research Center, Asan Medical Center (Korea). The samples were analyzed with an upright microscope (Zeiss, Germany), and the images were acquired under 400× magnification. The number of nuclei was quantitated in each mouse vessel. The experiments were performed in 5-6 independent replicates.

Reverse transcription-quantitative polymerase chain reaction (RT-qPCR)
The total RNA was isolated from HUVECs or mouse tissue using TRIzol Reagent solution (Ambion, USA). To estimate miR-34c expression, cDNAs were synthesized with predesigned Taqman probes (hsa-miR-34c or U6 snRNA) with a TaqMan MicroRNA assay kit (Applied Biosystems, USA) in accordance with the manufacturer's instructions; then, a QuantStudio 5 Real-time PCR system (Applied Biosystems) was used. Mature miR-34c expression was normalized to U6 snRNA, which served as an internal control.

To measure gene expression, DNase-treated total RNA was converted to cDNA using a Superscript III reverse transcriptase (Invitrogen, USA) and oligo dT primer (Invitrogen) according to the manufacturer's protocol. The cDNA was amplified with SYBR green master mix (Applied Biosystems). All primer sequences are listed in Supplementary Table S1. The relative quantities of *BCL2* or *HIF-1α* mRNA were normalized to both *HPRT* and *HuPO* expression, which were used as internal controls.

Luciferase reporter assay
The 3′ UTR region of *BCL2* (413 bp) was cloned into a psiCHECK-2 vector (Promega, USA). Then, an miR-34c binding site located in the *BCL2* 3′ UTR was mutated using a standard site-directed mutagenesis protocol. The primer sequences used in this study are listed in Supplementary Table S1. The luciferase plasmids were transfected into HEK293T cells using Lipofectamine 3000 (Invitrogen). After incubation for 24 h, luciferase activity was measured by performing a Dual-Glo luciferase assay (Promega) using a GloMax 96 microplate luminometer (Promega). After the Renilla luciferase activity

was normalized to the Firefly luciferase activity, the relative luciferase expression was normalized to that of the mutant sample.

Production of miR-34c-overexpressing HUVECs

For the overexpression of miR-34c, the human *MIR34C* flanking region was cloned into a lentiviral vector (pLVX-puro vector; Takara, Japan), as previously described (Kim et al., 2019). The pLVX-puro-miR-34c plasmids were cotransfected into HEK293T cells with psPAX2 (Gag-Pro-Plo) and pMD2. G (Env) using Lipofectamine 3000 (Invitrogen), according to the manufacturer's instructions. The supernatants containing lentivirus were harvested and filtrated through a 0.45-μm syringe filter unit (Millipore, USA) after 48 and 72 h. One day before lentivirus infection, HUVECs were seeded into tissue culture plates. After polybrene (Millipore) was added to the virus supernatants at 8 μg/ml, the culture media was replaced with the virus particle-containing media. The second infection was performed after 24 h of incubation. One day after the second infection, the cells were changed to fresh EGM-2 media and treated with and without H_2O_2 at 700 nM for dysoxia. The cells were harvested after 24 h of incubation for further assays.

For hypoxia by gas-induction, HUVECs were transduced by lentiviruses containing *MIR34C* at one day after the cells were seeded and cultured in a hypoxic chamber (1% O_2, 5% CO_2, and 90% N_2) for 72 h.

Caspase 3/7 and cell viability assays

HUVECs were seeded in 24-well plates and transduced by miR-34c-expressing lentivirus as described above. The cells were transferred to a 96-well white plate (Nunc, USA) in triplicate. For the inhibition of miR-34c, HUVECs were seeded and transfected with either an miR-34c inhibitor or a control (mirVana, USA) in the presence or absence of H_2O_2. After 24-48 h of incubation, the caspase 3/7 assays were conducted using a Caspase 3/7-glo assay kit (Promega). The activity of caspase 3/7 was measured using a GloMax 96 microplate luminometer (Promega).

To estimate the cell viability of miR-34c-overexpressing or inhibited HUVECs, the lentivirus-infected HUVECs or miR-34c inhibitor-transfected HUVECs were transferred to a 96-well transparent plate (Nunc), and a CCK-8 assay solution (Dojindo Molecular Technology, Japan) was added. After 3 h of incubation, the samples were measured at an absorbance of 450 nm with a microplate reader (Tecan, Switzerland).

Reactive oxygen species (ROS) assay

The cell lysates from control or miR-34c-overexpressing HUVECs under normoxia or hypoxia were prepared by homogenizing in PBS on ice. The ROS levels were determined by an OxiSelect[TM] *in vitro* ROS/RNS assay kit (Cell Biolabs, USA), according to the manufacturer's instructions. The fluorescence intensity was measured and analyzed at 480 nm excitation/530 nm emission using a fluorescence plate reader (Victor X3; PerkinElmer, USA).

Western blotting

Total cell lysates were prepared with RIPA buffer (Biosesang,

Korea) with a protease inhibitor cocktail (Roche, Switzerland). Protein samples were separated for 12%-15% sodium dodecyl sulfate polyacrylamide gel electrophoresis (SDS-PAGE) and transferred to a polyvinylidene difluoride (PVDF) membrane (GE Healthcare, USA). The membrane was incubated with primary antibodies to anti-BCL2 rabbit (Cell Signaling Technology, USA), anti-LC3B rabbit (Novus Biologicals, USA), anti-p62 mouse (Santa Cruz biotechnology, USA), anti-hypoxia-inducible factor (HIF)-1α mouse (Santa Cruz Biotechnology), anti-BAX rabbit (Cell Signaling Technology), and anti-β-actin rabbit (Bioss, USA) antibodies. The secondary antibodies were goat anti-rabbit IgG horseradish peroxidase (HRP)-conjugated (Santa Cruz Biotechnology) and goat anti-mouse IgG HRP-conjugated antibodies (Santa Cruz Biotechnology). Proteins were detected with enhanced chemiluminescence (ECL) solution (Pierce, USA) and analyzed with ImageQuant LAS 4000 (GE Healthcare). The band intensities were quantitated using ImageStudio Lite software (ver. 5.2; LI-COR Biosciences, USA).

Statistical analysis

All statistical analyses were performed with Student's *t*-test or one-way ANOVA with GraphPad Prism 6 (GraphPad Software, USA). Statistical significance is indicated by $*P < 0.05$ or $**P < 0.01$.

RESULTS

miR-34c is upregulated under hypoxic condition

To evaluate the expression of miR-34c under hypoxic condition *in vitro*, miR-34c levels were assessed in HUVEC lines under hypoxic conditions using a Taqman microRNA assay (Figs. 1A and 1B). To induce hypoxia to HUVEC lines, the cells were cultured in a chamber with 1% O_2 gas, or treated with H_2O_2, that has be commonly used as a phenocopy of hypoxic effects (Azimi et al., 2017; Han et al., 2018; Stegen et al., 2016). Nonetheless, when we treated H_2O_2, we call it as dysoxia for clarity. The expression of miR-34c was found to be significantly upregulated during hypoxia or dysoxia by approximately 5-fold and 1.7-fold, respectively, in 3 days (Figs. 1A and 1B). In addition, we adopted a murine HLI model to confirm whether miR-34c expression is also increased by hypoxia affecting the blood vessels *in vivo*. The expression of miR-34c was significantly increased in the ischemic vessels within 3 days, compared with the sham control (Fig. 1C). The expression of HIF-1α was increased when hypoxic/ischemic stress occurred (Supplementary Fig. S1). Collectively, these results suggest that miR-34c could be associated with the response to hypoxia.

Enhanced miR-34c expression promotes cell viability

Cell viability and apoptosis was assessed in miR-34c-overexpressing HUVECs, to investigate the effect of miR-34c on the response to hypoxia. Using a lentiviral system, miR-34c was dramatically overexpressed in HUVECs, and hypoxia further increased miR-34c expression over 10,000 folds (Supplementary Fig. S2A). The cell viability of miR-34c-overexpressing HUVECs was significantly elevated both in normoxia and in dysoxia (Fig. 2A). The caspase 3/7 activity was slightly in-
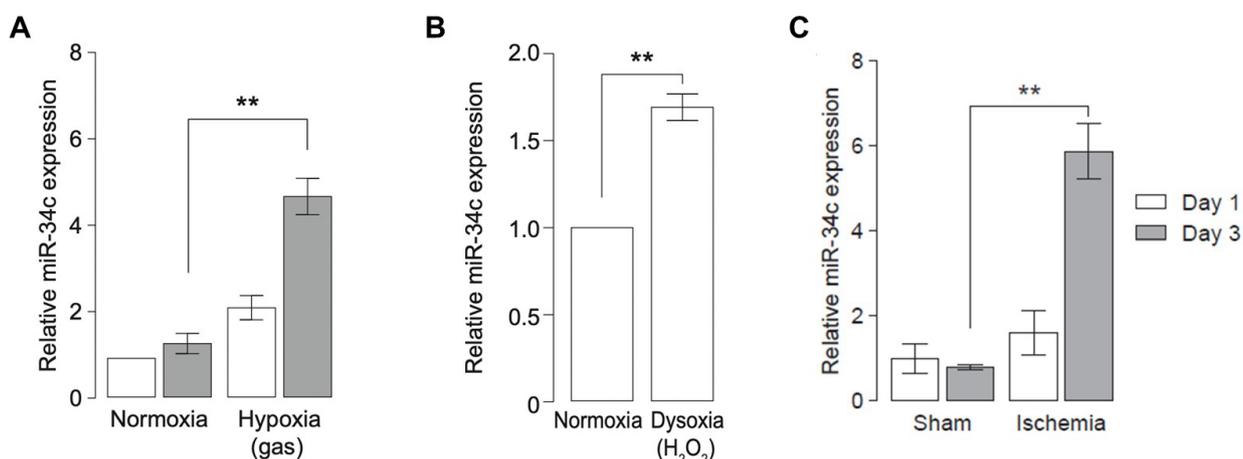
Fig. 1. Elevated expression of miR-34c in response to hypoxia both *in vitro* and *in vivo*. (A) The relative expression of miR-34c was evaluated by TaqMan microRNA assay in HUVEC lines under hypoxia by gas-induction (1% O_2) at day 1 (open bars) and 3 (gray bars). The graph shows mean ± SEM (normoxia: n = 3, hypoxia: n = 6). **$P < 0.01$. (B) The relative expression of miR-34c was evaluated by TaqMan microRNA assay in HUVEC lines under dysoxia by the treatment of hydrogen peroxide (H_2O_2) at day 3. Relative quantity of miR-34c in dysoxia was normalized to that of in normoxia control samples. n = 3; mean ± SD; **$P < 0.01$. (C) The relative expression of miR-34c was evaluated at day 1 (open bars) and day 3 (gray bars) in the veins from a mouse HLI model. n = 3; mean ± SD; **$P < 0.01$.
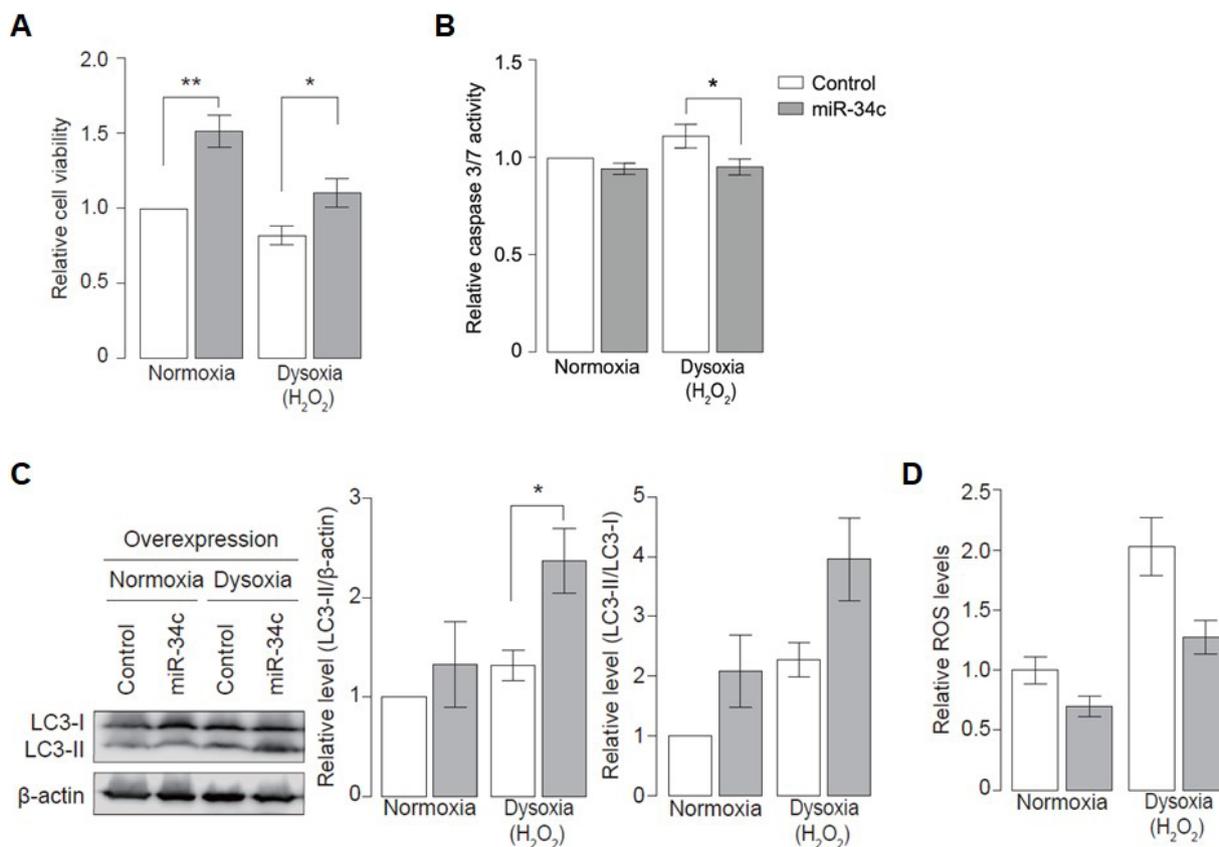
Fig. 2. Cellular apoptosis and proliferation regulated by miR-34c in hypoxia. (A) CCK-8 assay and (B) caspase 3/7 assay of miR-34c-overexpressing HUVECs with or without H_2O_2 treatment were conducted to estimate cell viability and caspase 3/7-mediated apoptosis, respectively. Cells were harvested at day 3 (n = 13-15; mean ± SEM; *$P < 0.05$, **$P < 0.01$). (C) Western blot analysis for LC3-I/II of LC3B isoform protein was performed to determine autophagy in H_2O_2-treated HUVECs. Quantitation of LC3-II expression was normalized to that of β-actin or LC3-I (n = 4; mean ± SEM; *$P < 0.05$). (D) Representative graph of the relative ROS levels in miR-34c-overexpressing HUVECs with or without H_2O_2 treatment. Mean ± SEM were displayed (n = 2). Control, empty vector (mock) control; miR-34c, miR-34c-overexpressing.

creased in the mock control by dysoxia, compared with normoxia, but when miR-34c was overexpressed, the increase was abolished (Fig. 2B). The decrease of caspase activity by miR-34c overexpression under dysoxia was statistically significant. The knockdown of miR-34c slightly increased caspase 3/7-mediated cell death regardless of hypoxia, while cell viability was not affected by miR-34c knockdown (Supplementary Figs. S2B and S2C). The results suggest that the expression of miR-34c might prevent hypoxic cells from apoptosis, resulting in increased cell survival.

As autophagy is essential for survival of hypoxic cells (Bellot et al., 2009; Zhang et al., 2008), autophagic activity was evaluated by the levels of LC3-II, an autophagy-associated form of LC3. The forced expression of miR-34c significantly promoted LC3-II expression in dysoxia groups compared with the mock control (Fig. 2C), indicating that autophagy was activated in miR-34c-overexpressing HUVECs treated with H_2O_2. Overexpression of miR-34c reduced ROS formation in HUVECs, implying that miR-34c expression could ameliorate hypoxic cellular damage (Fig. 2D). These data demonstrate that miR-34c enhanced cell viability by reducing apoptosis and inducing autophagy, reducing the cell damage caused by hypoxia.

BCL2 is a direct target of miR-34c, regulating autophagy

To understand the working mechanisms of miR-34c in response to hypoxia, we searched for potential targets for miR-34c using a bioinformatic algorithm tool (TargetScan
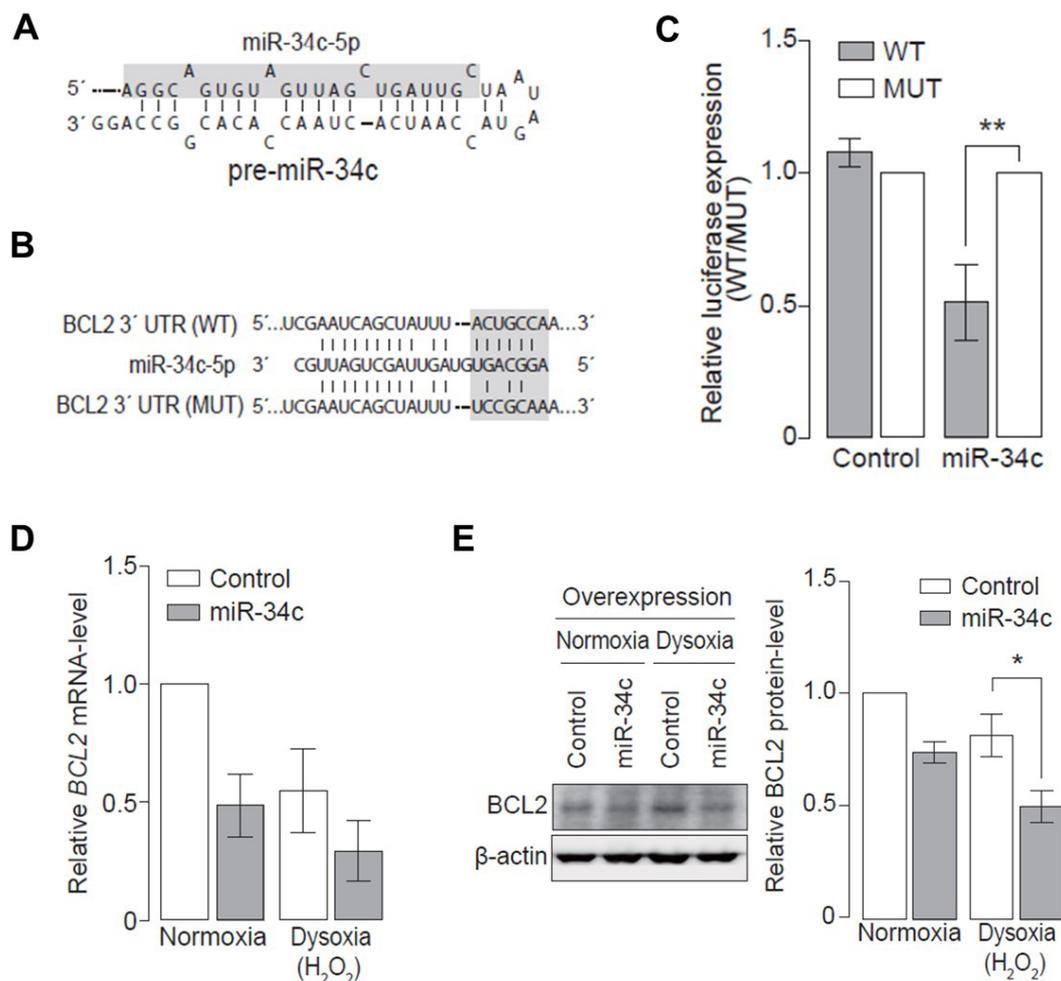
Fig. 3. BCL2 repressed by miR-34c directly. (A) The secondary structure of precursor miR-34c was predicted by the Mfold web server (mfold.rit.Albany.edu). The sequences of mature miR-34c-5p are highlighted in gray. (B) A target site of miR-34c-5p in BCL2 3′ UTR was predicted using the TargetScan prediction tool. The seed region is displayed in gray. Wild type (WT) represents the original sequences, whereas MUT represents the mutated seed sequences. (C) A luciferase reporter assay was performed in control or miR-34c-overexpressing HEK293T cells with psiCHECK-2 plasmids containing the WT or MUT sequences as described in (B). The relative luciferase expression of the plasmids with WT was normalized to those of MUT (n = 5; mean ± SEM; **P < 0.01). (D) The BCL2 mRNA levels were analyzed in miR-34c-overexpressing HUVEC by RT-qPCR. The mRNA levels of HuPO and HPRT were used as internal control. (E) The BCL2 protein levels were analyzed in miR-34c-overexpressing HUVEC by western blotting. β-Actin was used as a loading control. The band intensities of BCL2 were normalized to those of β-actin (n = 5; mean ± SEM; *P < 0.05). Control, empty vector (mock) control; miR-34c, miR-34c-overexpressing.

7.2) (Lee et al., 2020a). The potential target of miR-34c was *BCL2*, which is well-known to be associated with autophagy as well as apoptosis (Marino et al., 2014; Marquez and Xu, 2012) and suggested as a target gene of miR-34c previously (Li et al., 2018). Using the prediction tool, a putative binding site for miR-34c was identified in the 3′ UTR of *BCL2* (Fig. 3A). To confirm the *in silico* information, we examined the efficacy of miRNA targeting using a luciferase reporter assay. The luciferase activity was significantly lower in miR-34c-overexpressing cells than in control cells, while reduced luciferase activity was rescued by a mutation in the putative binding site of 3′ UTR of *BCL2* that could not bind with miR-34c (Figs. 3B and 3C). These results indicate that BCL2 expression is directly regulated by miR-34c. The effect of miR-34c expression on endogenous BCL2 expression was validated at both the mRNA and protein levels in HUVECs (Figs. 3D and 3E). These results show that overexpression of miR-34c repressed BCL2

mRNA and protein expression in HUVECs under hypoxic as well as normoxic conditions (Figs. 3D and 3E). The repression was significant in hypoxia. Thus, miR-34c directly inhibited BCL2 expression.

We further evaluated whether miR-34c-mediated BCL2 repression activates autophagic pathways. Autophagy was evaluated by p62 and LC3 levels in miR-34c-overexpressing HUVECs exposed to H_2O_2 (Fig. 4). We also measured p62 and LC3-II levels after treatment with chloroquine, an inhibitor of autophagosome-lysosomal fusion, as a positive control. Consistent with the results of Fig. 2C, the LC3 conversion (LC3-I to LC3-II) was significantly upregulated and p62 levels were also significantly downregulated in miR-34c-overexpressing HUVEC under dysoxic condition (Fig. 4). In addition, in response to hypoxia, overexpression of miR-34c inhibited BCL2 expression and activated autophagy by decreasing p62 and increasing LC3-II expression in HUVEC (Supplementary
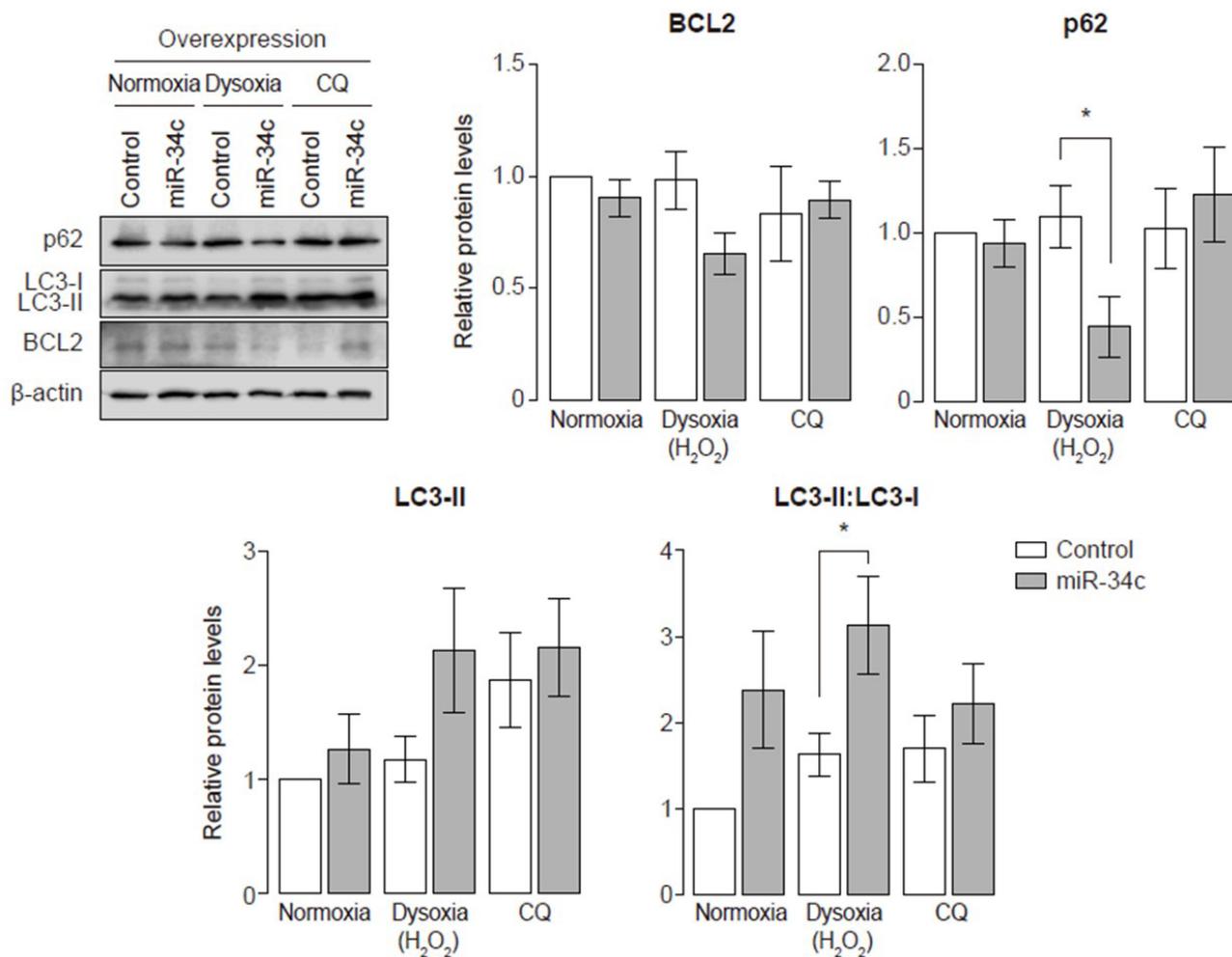
Fig. 4. Cellular autophagy induced by miR-34c in HUVECs upon hypoxia. The autophagy-related proteins, p62, and LC3-I/II of LC3B isoform were visualized by western blotting. β-Actin serves as a loading control. The expression of LC3-I/II, p62, and BCL2 were quantified and normalized to those of β-actin. Chloroquine (CQ) is an autophagy inhibitor that prevents autophagosome-lysosomal fusion, and HUVECs was treated with 20 μM CQ for 24 h. Relative protein levels to normoxia control were indicated in the graphs (BCL2, LC3B: n = 8, p62: n = 5; mean ± SEM; *$P < 0.05$). Control, empty vector (mock) control; miR-34c, miR-34c-overexpressed.

Fig. S3). The results suggest that downregulated BCL2 was accompanied with cellular autophagy.

miR-34c-mediated BCL2 repression has a protective effect against hypoxia *in vivo*

In light of the protective role of miR-34c in regulating BCL2 activity in response to hypoxia *in vitro* (Fig. 2D), we further examined the effect of BCL2 repression by miR-34c *in vivo* using a mouse HLI model. We injected lentivirus carrying the *MIR34C* gene into mice via their tail veins and assessed the protective effect on ischemic damage at day 3 (Fig. 5A). The viable cells in the vessels were stained by H&E and quantified by the number of nuclei. As seen in Fig. 5B, the ischemic vessels were less thick in the mice injected with miR-34c-expressing vector. The forced expression of miR-34c allowed approximately 30% more cells to survive in the hypoxic veins (Fig. 5B). Taken together, the ischemic damage was ameliorated in the blood vessels by miR-34c. The ischemic vessels where miR-34c was overexpressed showed repressed BCL2 expression. Furthermore, miR-34c-mediated BCL2 repression enhanced the activity of autophagy in response to ischemic damage of the vessels *in vivo* (Fig. 5C). These findings demonstrate that miR-34c inhibits BCL2 expression, promotes cellular autophagic activity, and reduces apoptosis, suggesting that miR-34c can have a protective function against hypoxic stress.

DISCUSSION

Herein we identified the role of miR-34c in autophagy and its protective function against hypoxia. miR-34c is a member of the miR-34 family, which consists miR-34a, miR-34b and miR-34c. Because the chromosomal loci of miR-34a and miR-34b/c are different, their functional activities can be differentially regulated relying on the molecular and cellular context despite miR-34s share the same seed sequences (Kim et al., 2019). miR-34c was significantly overexpressed in HUVECs upon induction of hypoxia and in hypoxic hindlimb vessels within 3 days. Consistently, miR-34c is significantly increased in hypoxic/ischemic injury to the rat liver via δ-opioid receptor activation (Zhi et al., 2017), and upregulated in mouse pulmonary smooth muscle cells under hypoxic conditions (Xu et al., 2012). The positive role of miR-34c in cell viability appeared to be rather intrinsic even without stimuli and help-
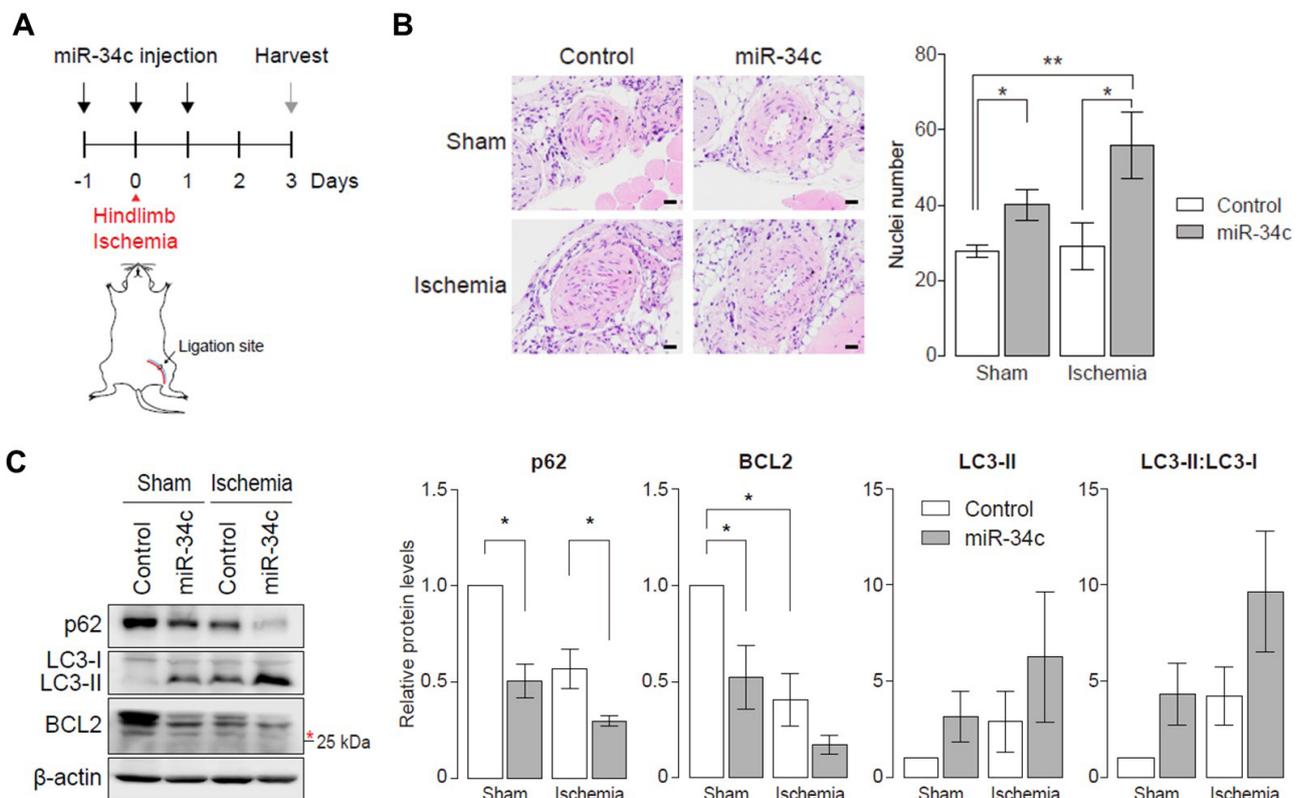
Fig. 5. miR-34c promotes autophagic activity *in vivo*. (A) Experimental scheme of miR-34c overexpression and mouse HLI. Lentiviruses carrying *MIR34C* gene were injected for 3 consecutive days via the tail veins. At day 0, HLI was established, and the vessels were harvested on day 3. (B) Representative images and quantitation of the number of nuclei in the H&E-stained mouse vessels. The arrows indicate the examples of living cells. The graph shows the mean ± SEM (sham control and miR-34c: n = 6, ischemia control: n = 5, ischemia miR-34c: n = 6; *P < 0.05, **P < 0.01). Scale bars = 20 μm. (C) Western blot analysis of autophagy markers (p62 and LC3-I/II) and BCL2 in the mouse vessels. An asterisk denotes the protein size of BCL2 (26 kDa). The size marker of 25 KDa is marked. β-Actin was used as a loading control. Quantitation of the proteins was normalized to β-actin, and the LC3-II/LC3-I ratio is indicated on the graph (mean ± SEM, n = 5; *P < 0.05). Control, empty vector (mock) control; miR-34c, miR-34c-overexpressing.

ful for HUVEC to survive under hypoxia. It is unlikely that the increase from the CCK8 assay was a result of increased proliferation, as miR-34c suppresses the proliferation of vascular smooth muscle cells (Choe et al., 2015).

We further investigated *BCL2* as a potential target of miR-34c, as BCL2 is associated with both apoptosis and autophagy (Fernandez et al., 2018; Marquez and Xu, 2012; Qi et al., 2015). As expected, the overexpression of miR-34c repressed the expression of BCL2, which was accompanied with decreased p62 and increased LC3-II *in vitro* ad *in vivo*. BCL2 is the BCL2 family protein that control cell survival primarily by direct binding their partner proteins, e.g., BAX and Beclin-1 (Kale et al., 2018), leading to either anti-apoptotic pathway or pro-apoptotic. BCL2 is known as not only an anti-apoptotic protein but also an anti-autophagic protein and acts as a toggle switch between apoptosis and autophagy (Marquez and Xu, 2012; Pattingre et al., 2005). Our data showed that miR-34c directly repressed BCL2 expression as well as that of BAX since a binding site of miR-34c exists on the BAX 3′ UTR, suggesting that the BAX/BCL2 ratio would not change (Supplementary Fig. S4A). As BAX/BCL2 ratio determines the apoptotic potential of a cell (Del Principe et al., 2016; Perlman et al., 1999), miR-34c-overexpression did not cause apoptosis but autophagy, consequently enhancing cell viability in HUVEC and the murine veins under hypoxic condition. We are aware that miR-34c induces apoptosis and decreases cell viability by repressing BCL2 in M4e laryngeal carcinoma cell lines (Li et al., 2018). The expression of miR-34c is highly enriched in adult murine testis and provokes germ cell apoptosis with the increase in BAX/BCL2 ratio by targeting ATF1 (Liang et al., 2012). In HeLa and SKOV3 cells, miR-34c targets ATG4B, and overexpressed miR-34c alone suppresses rapamycin-induced autophagy (Wu et al., 2017). This discrepancy could be explained that the cellular consequences of miR-34c/BCL2 axis might depend on cell types and stimulants such as hypoxic stress. In our study, HUVEC was primary, not immortalized, and we performed *in vivo* mouse HLI study to validate the results. It is broadly accepted that an individual miRNA can extensively regulate various transcripts (Baek et al., 2008; Selbach et al., 2008). Therefore, it is possible that the expression of miRNAs and their selection of target genes depend on the cell types, stimulants, and timing. For instances, the regulation of target genes is finely tuned by miRNAs during developmental stages (Bushati and Cohen, 2007).

Interacting with Beclin-1, BCL2 prevents autophagic activity (Fernandez et al., 2018; Glick et al., 2010; Qi et al., 2015). Several studies described that BCL2 function appears to be dependent on the intracellular localization such as endoplasmic reticulum (ER) and mitochondria. ER-localized BCL2 can inhibit autophagy, while mitochondrial BCL2 cannot (Decuypere et al., 2012). A possible explanation is that the BCL2/Beclin-1 complex is mainly present at the ER membranes under cellular stresses (Maiuri et al., 2007). Our results showed that the inhibition of BCL2 expression by miR-34c activated cellular autophagy in HUVEC lines and a mouse HLI model. In line with our observation, a recent paper uncovered that disruption of the Beclin-1 and BCL2 interaction by phosphorylation of BCL2 induces autophagy in limb remote ischemic conditioned rats (Qi et al., 2015). Therefore, reduced BCL2

expression could induce autophagy by disrupting BCL2/Beclin-1 interaction, following the upregulation of miR-34c upon hypoxia.

In our current study, forced expression of miR-34c activated cellular autophagy and reduced ROS in HUVEC lines under hypoxia, strongly supporting that miR-34c-stimulated autophagy has a protective effect on the hypoxic stress-induced cells. However, there are other miRNAs involved in ischemic injury and autophagy. miR-26a plays a protective role in ischemic myocardial injury in mice by regulating autophagy through Usp15 (Liang et al., 2020). In addition, miR-15 and miR-16 target BCL2 (Pekarsky et al., 2018), although miR-15 and miR-16 are downregulated in hypoxia (Nallamshetty et al., 2013). Overexpressed miR-372 blcoks autophagy through p62 upon starvation (Feng et al., 2014). Thus, we cannot exclude the possibility that multiple miRNAs could cooperate to induce autophagy in response to hypoxia, resulting in ameliorating ischemic injury.

In accordance with our current study, miR-34c expression was slightly higher in the biopsy samples collected from patients with CAV 1-month post-operatively than in those from healthy control subjects (Supplementary Materials and Methods, Supplementary Table S2, Supplementary Fig. S4B). CAV, an accelerated form of coronary artery disease, is a main limiting factor for the long-term survival of the cardiac transplant patients (Pighi et al., 2020; Schmauss and Weis, 2008; Singh et al., 2015). Although cardiac transplantation is the last chance for patients with end-stage heart failure, the incidence rate of CAV progressively increases up to 50% at 10 years postoperatively (Pighi et al., 2020). However, the diagnosis of CAV is limited and difficult to recognize at the early CAV development due to the lack of clinical symptoms for ischemia (Schmauss and Weis, 2008). Therefore, it is essential to identify the noninvasive biomarkers that detect CAV. Along with miR-34a and miR-34b, miR-34c is upregulated in the mouse heart by transverse aortic constriction, suggested as a therapeutic target (Bernardo et al., 2012). In our unpublished preliminary miRNA microarray study, miR-34c expression, but not miR-34a, was elevated in a CAV patient sample compared with healthy control. The results suggest that miR-34c could be a diagnostic biomarker of CAV. However, it awaits further investigations to reveal the mechanisms of miR-34c directly involved in CAV development, as well as clinical studies with larger cohorts.

In conclusion, BCL2 was directly repressed by miR-34c, resulting in cellular autophagy in HUVEC and mouse blood vessels under conditions of hypoxic/ischemic stress both *in vitro* and *in vivo*. As results, miR-34c played a protective role in cellular viability of HUVEC upon hypoxia and in a murine HLI model. Our present study suggests the role of miR-34c in autophagy and provides insight on the protective effects of miR-34c in response to hypoxia.

Note: Supplementary information is available on the Molecules and Cells website (www.molcells.org).

AUTHOR CONTRIBUTIONS

S.K. conducted the research, analyzed the results, and wrote the manuscript. J.H. conducted the research and analyzed the results. Y.-H.A., C.H.H., and J.J.H. provided materials and discussed the results. S.-E.L. provided materials and analyzed the results. J.-J.K. conceptualized the research and obtained the grants. N.K. conceptualized and conducted the research, analyzed and discussed the results, and wrote the manuscript.

CONFLICT OF INTEREST

The authors have no potential conflicts of interest to disclose.

ORCID

Soyoung Kim   https://orcid.org/0000-0002-3181-1290
Jaeseok Han   https://orcid.org/0000-0002-0033-6300
Young-Ho Ahn   https://orcid.org/0000-0002-1084-0367
Chang Hoon Ha   https://orcid.org/0000-0001-7606-4340
Jung Jin Hwang   https://orcid.org/0000-0003-0912-1055
Sang-Eun Lee   https://orcid.org/0000-0002-7290-2463
Jae-Joong Kim   https://orcid.org/0000-0002-2714-2282
Nayoung Kim   https://orcid.org/0000-0001-8598-0068

REFERENCES

Akkoc, Y. and Gozuacik, D. (2020). MicroRNAs as major regulators of the autophagy pathway. Biochim. Biophys. Acta Mol. Cell Res. *1867*, 118662.

Azimi, I., Petersen, R.M., Thompson, E.W., Roberts-Thomson, S.J., and Monteith, G.R. (2017). Hypoxia-induced reactive oxygen species mediate N-cadherin and SERPINE1 expression, EGFR signalling and motility in MDA-MB-468 breast cancer cells. Sci. Rep. *7*, 15140.

Baek, D., Villen, J., Shin, C., Camargo, F.D., Gygi, S.P., and Bartel, D.P. (2008). The impact of microRNAs on protein output. Nature *455*, 64-71.

Bellot, G., Garcia-Medina, R., Gounon, P., Chiche, J., Roux, D., Pouyssegur, J., and Mazure, N.M. (2009). Hypoxia-induced autophagy is mediated through hypoxia-inducible factor induction of BNIP3 and BNIP3L via their BH3 domains. Mol. Cell. Biol. *29*, 2570-2581.

Bernardo, B.C., Gao, X.M., Winbanks, C.E., Boey, E.J., Tham, Y.K., Kiriazis, H., Gregorevic, P., Obad, S., Kauppinen, S., Du, X.J., et al. (2012). Therapeutic inhibition of the miR-34 family attenuates pathological cardiac remodeling and improves heart function. Proc. Natl. Acad. Sci. U. S. A. *109*, 17615-17620.

Bushati, N. and Cohen, S.M. (2007). microRNA functions. Annu. Rev. Cell Dev. Biol. *23*, 175-205.

Chen, Z., Lai, T.C., Jan, Y.H., Lin, F.M., Wang, W.C., Xiao, H., Wang, Y.T., Sun, W., Cui, X., Li, Y.S., et al. (2013). Hypoxia-responsive miRNAs target argonaute 1 to promote angiogenesis. J. Clin. Invest. *123*, 1057-1067.

Choe, N., Kwon, J.S., Kim, Y.S., Eom, G.H., Ahn, Y.K., Baik, Y.H., Park, H.Y., and Kook, H. (2015). The microRNA miR-34c inhibits vascular smooth muscle cell proliferation and neointimal hyperplasia by targeting stem cell factor. Cell. Signal. *27*, 1056-1065.

Decuypere, J.P., Parys, J.B., and Bultynck, G. (2012). Regulation of the autophagic bcl-2/beclin 1 interaction. Cells *1*, 284-312.

Del Principe, M.I., Dal Bo, M., Bittolo, T., Buccisano, F., Rossi, F.M., Zucchetto, A., Rossi, D., Bomben, R., Maurillo, L., Cefalo, M., et al. (2016). Clinical significance of bax/bcl-2 ratio in chronic lymphocytic leukemia.

Haematologica *101*, 77-85.

Feng, L., Ma, Y., Sun, J., Shen, Q., Liu, L., Lu, H., Wang, F., Yue, Y., Li, J., Zhang, S., et al. (2014). YY1-MIR372-SQSTM1 regulatory axis in autophagy. Autophagy *10*, 1442-1453.

Fernandez, A.F., Sebti, S., Wei, Y., Zou, Z., Shi, M., McMillan, K.L., He, C., Ting, T., Liu, Y., Chiang, W.C., et al. (2018). Disruption of the beclin 1-BCL2 autophagy regulatory complex promotes longevity in mice. Nature *558*, 136-140.

Glick, D., Barth, S., and Macleod, K.F. (2010). Autophagy: cellular and molecular mechanisms. J. Pathol. *221*, 3-12.

Guo, F., Tang, C., Huang, B., Gu, L., Zhou, J., Mo, Z., Liu, C., and Liu, Y. (2022). LncRNA H19 drives proliferation of cardiac fibroblasts and collagen production via suppression of the miR-29a-3p/miR-29b-3p-VEGFA/TGF-beta axis. Mol. Cells *45*, 122-133.

Gurusamy, N., Lekli, I., Gorbunov, N.V., Gherghiceanu, M., Popescu, L.M., and Das, D.K. (2009). Cardioprotection by adaptation to ischaemia augments autophagy in association with BAG-1 protein. J. Cell. Mol. Med. *13*, 373-387.

Gustafsson, A.B. and Gottlieb, R.A. (2009). Autophagy in ischemic heart disease. Circ. Res. *104*, 150-158.

Han, F., Li, C.F., Cai, Z., Zhang, X., Jin, G., Zhang, W.N., Xu, C., Wang, C.Y., Morrow, J., Zhang, S., et al. (2018). The critical role of AMPK in driving Akt activation under stress, tumorigenesis and drug resistance. Nat. Commun. *9*, 4728.

Jang, K.H., Hwang, Y., and Kim, E. (2020). PARP1 impedes SIRT1-mediated autophagy during degeneration of the retinal pigment epithelium under oxidative stress. Mol. Cells *43*, 632-644.

Kale, J., Osterlund, E.J., and Andrews, D.W. (2018). BCL-2 family proteins: changing partners in the dance towards death. Cell Death Differ. *25*, 65-80.

Kim, J.S., Kim, E.J., Lee, S., Tan, X., Liu, X., Park, S., Kang, K., Yoon, J.S., Ko, Y.H., Kurie, J.M., et al. (2019). MiR-34a and miR-34b/c have distinct effects on the suppression of lung adenocarcinomas. Exp. Mol. Med. *51*, 1-10.

Lee, H.E., Park, S.J., Huh, J.W., Imai, H., and Kim, H.S. (2020a). Enhancer function of microRNA-3681 derived from long terminal repeats represses the activity of variable number tandem repeats in the 3' UTR of SHISA7. Mol. Cells *43*, 607-618.

Lee, P., Chandel, N.S., and Simon, M.C. (2020b). Cellular adaptation to hypoxia through hypoxia inducible factors and beyond. Nat. Rev. Mol. Cell Biol. *21*, 268-283.

Li, R., Zhang, H., and Zheng, X. (2018). MiR-34c induces apoptosis and inhibits the viability of M4e cells by targeting BCL2. Oncol. Lett. *15*, 3357-3361.

Liang, H., Su, X., Wu, Q., Shan, H., Lv, L., Yu, T., Zhao, X., Sun, J., Yang, R., Zhang, L., et al. (2020). LncRNA 2810403D21Rik/Mirf promotes ischemic myocardial injury by regulating autophagy through targeting Mir26a. Autophagy *16*, 1077-1091.

Liang, X., Zhou, D., Wei, C., Luo, H., Liu, J., Fu, R., and Cui, S. (2012). MicroRNA-34c enhances murine male germ cell apoptosis through targeting ATF1. PLoS One *7*, e33861.

Liu, W.J., Ye, L., Huang, W.F., Guo, L.J., Xu, Z.G., Wu, H.L., Yang, C., and Liu, H.F. (2016). p62 links the autophagy pathway and the ubiquitin-proteasome system upon ubiquitinated protein degradation. Cell. Mol. Biol. Lett. *21*, 29.

Maiuri, M.C., Le Toumelin, G., Criollo, A., Rain, J.C., Gautier, F., Juin, P., Tasdemir, E., Pierron, G., Troulinaki, K., Tavernarakis, N., et al. (2007). Functional and physical interaction between Bcl-X(L) and a BH3-like domain in Beclin-1. EMBO J. *26*, 2527-2539.

Marino, G., Niso-Santano, M., Baehrecke, E.H., and Kroemer, G. (2014). Self-consumption: the interplay of autophagy and apoptosis. Nat. Rev. Mol. Cell Biol. *15*, 81-94.

Marquez, R.T. and Xu, L. (2012). Bcl-2:Beclin 1 complex: multiple, mechanisms regulating autophagy/apoptosis toggle switch. Am. J. Cancer Res. *2*, 214-221.

Michiels, C. (2004). Physiological and pathological responses to hypoxia. Am. J. Pathol. *164*, 1875-1882.

Mizushima, N., Yoshimori, T., and Levine, B. (2010). Methods in mammalian autophagy research. Cell *140*, 313-326.

Nallamshetty, S., Chan, S.Y., and Loscalzo, J. (2013). Hypoxia: a master regulator of microRNA biogenesis and activity. Free Radic. Biol. Med. *64*, 20-30.

Pattingre, S., Tassa, A., Qu, X., Garuti, R., Liang, X.H., Mizushima, N., Packer, M., Schneider, M.D., and Levine, B. (2005). Bcl-2 antiapoptotic proteins inhibit Beclin 1-dependent autophagy. Cell *122*, 927-939.

Pekarsky, Y., Balatti, V., and Croce, C.M. (2018). BCL2 and miR-15/16: from gene discovery to treatment. Cell Death Differ. *25*, 21-26.

Perlman, H., Zhang, X., Chen, M.W., Walsh, K., and Buttyan, R. (1999). An elevated bax/bcl-2 ratio corresponds with the onset of prostate epithelial cell apoptosis. Cell Death Differ. *6*, 48-54.

Pighi, M., Gratta, A., Marin, F., Bellamoli, M., Lunardi, M., Fezzi, S., Zivelonghi, C., Pesarini, G., Tomai, F., and Ribichini, F. (2020). "Cardiac allograft vasculopathy: pathogenesis, diagnosis and therapy". Transplant. Rev. (Orlando) *34*, 100569.

Qi, Z., Dong, W., Shi, W., Wang, R., Zhang, C., Zhao, Y., Ji, X., Liu, K.J., and Luo, Y. (2015). Bcl-2 phosphorylation triggers autophagy switch and reduces mitochondrial damage in limb remote ischemic conditioned rats after ischemic stroke. Transl. Stroke Res. *6*, 198-206.

Schmauss, D. and Weis, M. (2008). Cardiac allograft vasculopathy: recent developments. Circulation *117*, 2131-2141.

Selbach, M., Schwanhausser, B., Thierfelder, N., Fang, Z., Khanin, R., and Rajewsky, N. (2008). Widespread changes in protein synthesis induced by microRNAs. Nature *455*, 58-63.

Singh, N., Heggermont, W., Fieuws, S., Vanhaecke, J., Van Cleemput, J., and De Geest, B. (2015). Endothelium-enriched microRNAs as diagnostic biomarkers for cardiac allograft vasculopathy. J. Heart Lung Transplant. *34*, 1376-1384.

Stegen, S., van Gastel, N., Eelen, G., Ghesquiere, B., D'Anna, F., Thienpont, B., Goveia, J., Torrekens, S., Van Looveren, R., Luyten, F.P., et al. (2016). HIF-1alpha promotes glutamine-mediated redox homeostasis and glycogen-dependent bioenergetics to support postimplantation bone cell survival. Cell Metab. *23*, 265-279.

Tan, Q., Wang, M., Yu, M., Zhang, J., Bristow, R.G., Hill, R.P., and Tannock, I.F. (2016). Role of autophagy as a survival mechanism for hypoxic cells in tumors. Neoplasia *18*, 347-355.

Wu, Y., Dai, X., Ni, Z., Yan, X., He, F., and Lian, J. (2017). The downregulation of ATG4B mediated by microRNA-34a/34c-5p suppresses rapamycin-induced autophagy. Iran. J. Basic Med. Sci. *20*, 1125-1130.

Xu, X., Wang, S., Liu, J., Dou, D., Liu, L., Chen, Z., Ye, L., Liu, H., He, Q., Raj, J.U., et al. (2012). Hypoxia induces downregulation of soluble guanylyl cyclase beta1 by miR-34c-5p. J. Cell Sci. *125*, 6117-6126.

Zhang, H., Bosch-Marce, M., Shimoda, L.A., Tan, Y.S., Baek, J.H., Wesley, J.B., Gonzalez, F.J., and Semenza, G.L. (2008). Mitochondrial autophagy is an HIF-1-dependent adaptive metabolic response to hypoxia. J. Biol. Chem. *283*, 10892-10903.

Zhi, F., Shao, N., Xue, L., Xu, Y., Kang, X., Yang, Y., and Xia, Y. (2017). Characteristic microRNA expression induced by delta-opioid receptor activation in the rat liver under prolonged hypoxia. Cell. Physiol. Biochem. *44*, 2296-2309.

Zhou, L., Zang, G., Zhang, G., Wang, H., Zhang, X., Johnston, N., Min, W., Luke, P., Jevnikar, A., Haig, A., et al. (2013). MicroRNA and mRNA signatures in ischemia reperfusion injury in heart transplantation. PLoS One *8*, e79805.